Transparent and Printable Regenerated Kenaf Cellulose/PVA Film

Hatika Kaco,[a] Sarani Zakaria,[a,]* Chin Hua Chia,[a] and Lina Zhang [b]

Cellulose was extracted from kenaf core powder by a series of bleaching processes and subsequently dissolved using an alkaline LiOH/urea solvent at low temperatures. The produced cellulose solution was mixed with polyvinyl alcohol (PVA) with different ratios of cellulose/PVA and coagulated to produce regenerated transparent films. The films were then air dried to produce transparent film. The effects of PVA content on tensile index, transparency, pore size, and printability of the films were studied. A slight reduction of 7% on the tensile index of the film was observed when the content of PVA increased to 10%. Nevertheless, the addition of 10% of PVA increased the porosity of the regenerated cellulose/PVA film, while the transparency of the film increased by 10%. The films were color-printed using a laser printer and can be recycled, in which the printed ink can be removed easily from the films with higher amount of PVA content. In addition, the films can be reprinted repeatedly several times.

Keywords: Reprint; Ink adhesion; Porosity; Film

*Contact information: a: School of Applied Physics, Faculty of Science and Technology, Universiti Kebangsaan Malaysia, 43600 UKM Bangi, Selangor, Malaysia; b: Department of Chemistry, Wuhan University, Wuhan 430072, China; *Corresponding author: sarani@ukm.my*

INTRODUCTION

Kenaf (*Hibiscus cannabinus* L.) is an important, fast-growing, short-term, annual industrial crop cultivated in most regions of the world (Chia *et al.* 2008; Wang *et al.* 2010; Chiaiese *et al.* 2011). Kenaf stem consists of an outer part (bark), comprising 35 to 40% of the stem, and the remaining portion is the inner part (core) (Abdul Khalil *et al.* 2010; Wang *et al.* 2010). Since the 1960s, kenaf has been selected by the U.S. Department of Agriculture as an annual crop source of fiber for pulp and paper making (Mambelli and Grandi 1995). The Market potential of kenaf has increased due to the increase in the cultivation of kenaf. Hence, several investigations have studied the potential of kenaf for the pulp and paper industry (Wang *et al.* 2010).

Cellulose is the most abundant biopolymer on Earth and is a valuable renewable, biodegradable, and bio-compatible natural resource (Luo and Zhang 2013). It consists of anhydroglucose units, linked by β-1,4-D-glycosidic bonds. Cellulose is hydrophilic in nature and tends to absorb a high proportion of water due to the large number of hydroxyl groups (Luo and Zhang 2013). A new environmentally friendly solvent, consisting of alkaline (LiOH or NaOH) and urea, was developed to dissolve cellulose at low temperature (Zhang *et al.* 2010a). The dissolved cellulose can be further regenerated into various forms such as hydrogel, films, membranes, and beads (Jin *et al.* 2007).

Mixing of cellulose with synthetic polymers has been developed intensively for different purposes. Yang *et al.* (1999) reported the preparation of films from cellulose

and polyethylene glycol (PEG) using PEG with different molecular weights. The study found that the increase of the molecular weight of PEG increased the crystallinity, while the miscibility of the mixture was decreased. In another study, polylactic acid (PLA) was mixed with microfibrillated cellulose (MFC) to increase the thermal and mechanical properties of the products (Suryanegara *et al.* 2009). Cellulose has also been used to reinforce PLA films to enhance the mechanical properties of the samples (Graupner *et al.* 2009).

Polyvinyl alcohol (PVA) is a biocompatible petroleum-based polymer. It is also one of the rare polymers with a carbon–carbon single bond backbone that is fully biodegradable. Because of the hydroxyl (−OH) groups on the alternating carbon atoms, PVA is strongly hydrophilic and soluble in water, which promotes its degradation through hydrolysis. In addition, OH groups in PVA are expected to form hydrogen bonds and acetal linkages with other materials, such as cellulose and aldehydes (Qiu and Netravali 2012). The hydrogen bonds between OH groups play an important role in determining the properties of PVA, such as water solubility, crystallinity range, and crystal modulus (Pawde *et al.* 2008).

In this study, a cellulose solution (CS), obtained by dissolving kenaf core cellulose, was mixed with PVA. The mixture was cast and regenerated to form transparent regenerated cellulose film. The aim of this study is to evaluate the effects of PVA content in cellulose solutions on the properties of the film, *i.e.*, pore size, transparency, tensile strength, and printability.

EXPERIMENTAL

Materials

Kenaf core (KC) powder was supplied by the Malaysian Agricultural Research and Development Institute (MARDI). Analytical grade sodium hydroxide (NaOH), lithium hydroxide monohydrate ($LiOH{\cdot}H_2O$), urea, sulfuric acid (H_2SO_4), and polyvinyl alcohol (PVA) with a molecular weight of 85,000 to 146,000 were purchased from Sigma Aldrich.

Method

Cellulose extraction

The KC powder (60- to 80-mesh) was bleached (D) to remove the lignin by using acetate buffered aqueous chlorite (1.7% w/v). Alkali treatment (E) was conducted using 2% NaOH at 80 °C for 2 h, and the process was repeated for seven stages (DEDEDED). The KC powder was dried at 105 °C for 24 h and kept in a desiccator for further use. The viscosity average molecular weight (M_η) of the KC is 1.68×10^5, which was determined using an Ubbelohde viscometer in cadoxen at 25 °C (Cai *et al.* 2006).

Preparation of cellulose/PVA films

An aqueous LiOH/urea solution at a weight ratio of 4.6:15 was prepared and stored at −13 °C in a freezer. The bleached KC cellulose powder (3 wt%) was added to the LiOH/urea solution and stirred for 5 min. The solution was frozen again in the freezer at −13 °C, and this process was repeated three times. The frozen solid was thawed and stirred extensively at room temperature to obtain a transparent cellulose solution. The

transparent solution was centrifuged at 12,000 rpm for 5 min to remove gas bubbles and separate the dissolved and undissolved cellulose. A PVA solution was prepared by dissolving PVA powder in distilled water at 90 °C for 4 h to obtain a 4 wt% PVA aqueous solution.

Cellulose/PVA (CS/PVA) solutions were prepared at different ratios, *i.e.*, 99/1, 95/5, and 90/10 (w/w), coded as PVA1, PVA5, and PVA10, respectively. The CS/PVA solution was stirred for 30 min and centrifuged for 1 min at 8000 rpm to remove gas bubbles. Then, the solution was cast on a glass plate and coagulated in a H_2SO_4 solution (5%) in which one surface contacted the glass slide (bottom side) and the other one directly contacted the coagulant bath (top side) to form the CS/PVA film. The film was washed with distilled water to remove excess chemicals and air dried on a poly(methyl methacrylate) sheet for further characterization.

The surface morphology of the films was studied using a scanning electron microscope (SEM LEO 1450VP). The sample was sputter-coated with gold before the observation. The film samples were analyzed using attenuated total reflectance-Fourier transform infrared spectroscopy (ATR-FTIR) and X-ray diffraction (XRD). The transparency of films prepared from different CS/PVA ratios was measured by a UV-visible spectrophotometer (Jenway 7315) at wavelengths ranging from 200 to 800 nm, in which the thickness of the films was approximately 0.015 mm. The tensile properties of films with different CS/PVA ratios were measured using a tensile machine (Buchel Van Der Korput Horizontal Tensile Tester model 086) at a speed of 10 mm min^{-1}. The samples were cut to a size of 50 × 10 mm, and three replicates were performed for each sample. The films were laser-printed (HP Laserjet CP1515n) on the top side of the films surface, and the strength of the ink adhesion was determined according to the ASTM F2252-03 standard method. The test was performed using Scotch Magic tape (3M, USA). Briefly, a piece of tape was stacked on the printed area on the film and lifted off with consistent force at an angle of 90°. The ink on the printed film was removed by immersion in distilled water at room temperature. The film was printed again three times to observe their printability.

RESULTS AND DISCUSSION

FTIR and XRD Characterizations

Figure 1 shows the IR spectra of neat regenerated cellulose, neat PVA, and CS/PVA films at different PVA contents. The broad absorption band observed ranging from 3200 to 3500 cm^{-1} for cellulose, cellulose mixed PVA, and neat PVA corresponds to OH stretching due to the presence of hydrogen bonds (Fortunati *et al.* 2013; Qiu *et al.* 2012). The intensity of the band increased as the PVA content increased, revealing the greater hydrogen bonding between cellulose and PVA (Gupta *et al.* 2013). The intensity of the absorption peak at 2929 cm^{-1} is due to the C−H stretching in cellulose, while the bands in the 1615 cm^{-1} region for cellulose may be attributed to C=O stretching vibrations. The bands observed from 1446 to 1346 cm^{-1} are associated with C−H in the plane deformation of C−H groups (Ibrahim *et al.* 2013). The band that occurred at 1160 cm^{-1} belongs to the C−O stretching of cellulose (Wu *et al.* 2009). The peak ranging from 894 to 902 cm^{-1} is due to β-glucosidic linkage (Zhang *et al.* 2002; Ibrahim *et al.* 2013). In this specific range, the increase of PVA content in the cellulose had a slight effect on the

intensity for all peaks, as the intensity peaks for all samples reduced as the PVA content in the CS/PVA film increased, for all spectra from (a) to (d).

For the neat PVA, the same intensity peaks were observed as were seen for cellulose and CS/PVA peaks in the range of 3200 to 3500 cm^{-1}. The peak at 1490 to 1340 cm^{-1} corresponds to C−H stretching. A sharp band at 1178 cm^{-1} corresponds to an acetyl C−O group present on the PVA backbone. The presence of these bands is attributed to the dispersion of the dissolved cellulose fiber in the mixed polymer (Ibrahim *et al.* 2013). However, the addition of PVA in cellulose up to 10% still does not contribute to significant IR signals of PVA peaks in the films. This is because the amount of PVA was insufficient in the sample for the signal to be observed.

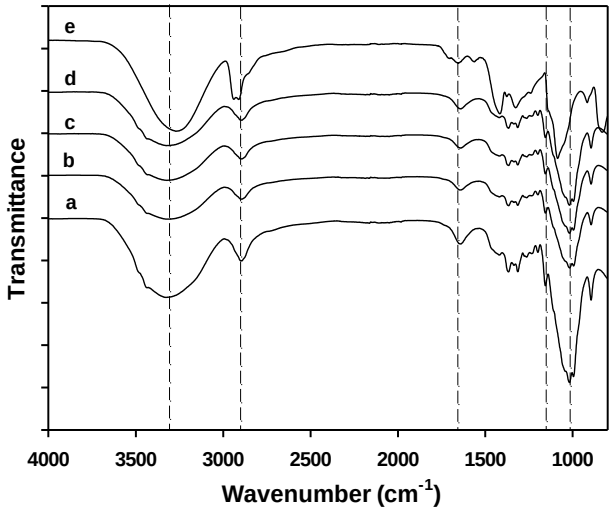

Fig. 1. ATR-FTIR of films (a) PVA0, (b) PVA1, (c) PVA5, (d) PVA10, and (e) PVA

Figure 2 shows the XRD patterns of the cellulose/PVA films at different PVA contents.

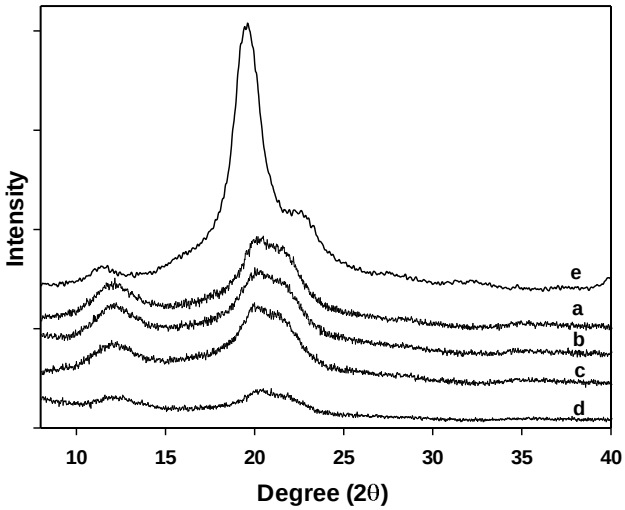

Fig. 2. XRD patterns of (a) PVA0, (b) PVA1, (c) PVA5, (d) PVA10, and (e) PVA

All the cellulose/PVA film samples exhibited a crystalline structure, showing diffraction peaks at 2θ = 12.4°, 20.3°, and 22.2°, which can be assigned to the cellulose II crystal planes (1 $\bar{1}$ 0), (1 1 0), and (2 0 0), respectively. These films differed from native cellulose, in which the crystal planes (1 $\bar{1}$ 0), (1 1 0), (2 0 0), and (0 0 4) exhibited diffraction peaks at 2θ = 14.9°, 16.3°, 22.6°, and 34.5°, which can be assigned to cellulose I (Li *et al.* 2012). This indicates that native cellulose, which is cellulose I, has been transformed into the cellulose II crystal state. Figure 2(e) shows the XRD pattern for neat PVA where the crystalline peaks were at 11.4° and 19.6°, which correspond to PVA crystalline phase (Roy and Bysakh 2011). The crystallinity index (CrI) of the cellulose/PVA film decreased with increasing PVA content. This can be attributed to the presence of PVA in the cellulose solution destroying the ordered packing of the mixed polymer. In addition, the overlapping of cellulose and PVA peaks occurred, leading to the decrease in the diffraction intensity.

Surface Morphology

Figures 3 and 4 show the morphology of the top side (contacting the coagulant) and bottom side (contacting the glass plate) of films with different CS/PVA ratios. As illustrated in Fig. 3, the porosity of the film's surface increased with increasing PVA content. This is due to greater interaction between the PVA and cellulose *via* hydrogen bonds between cellulose chains and hydroxyl groups (−OH) from PVA, while the other bonds formed between secondary OH at C2 or C3 with OH in PVA (Sawatari and Kondo 1999).

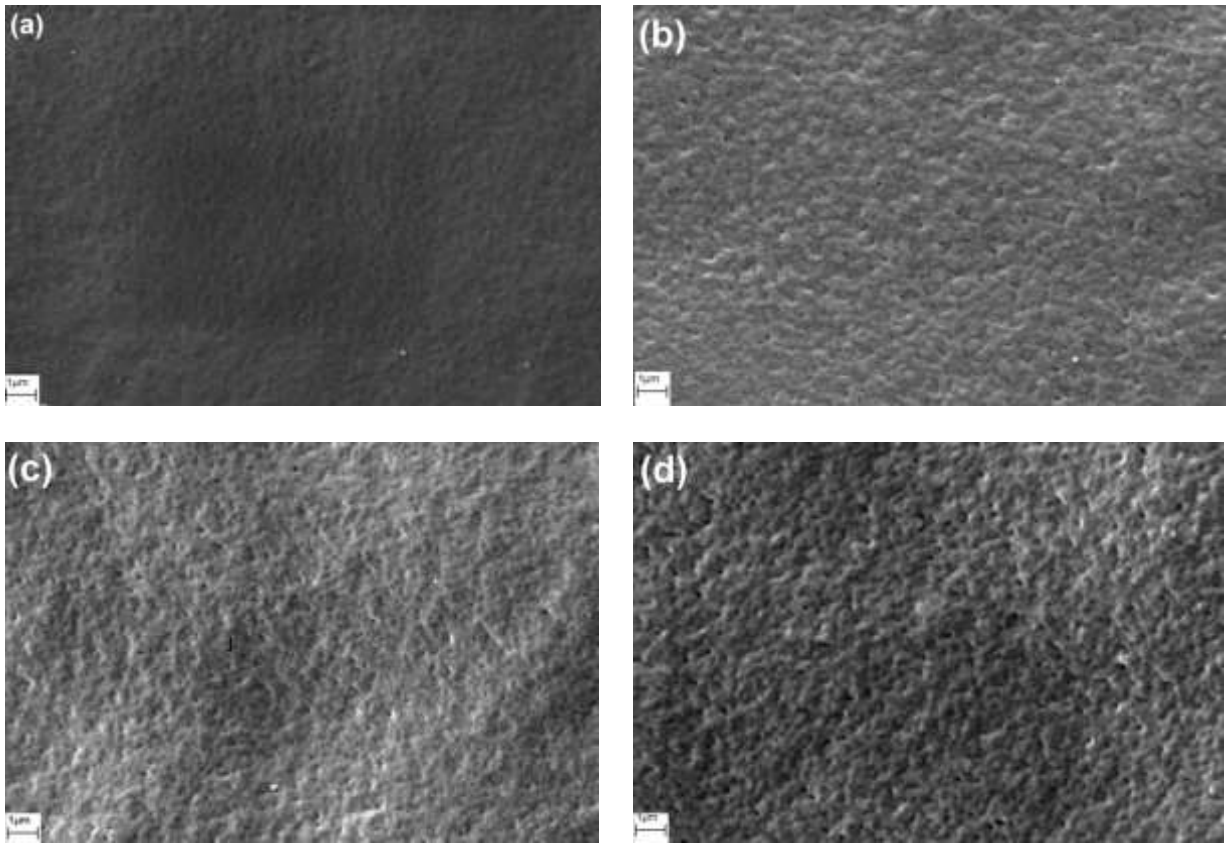

Fig. 3. SEM images of the top side of films (a) PVA0, (b) PVA1, (c) PVA5, and (d) PVA10

Figures 4(a) to (d) show a smooth surface. Contact between the cellulose solution and the glass plate contributed to the smooth and low porosity of the film's surface. In addition, the diffusion of acid during the coagulation process was slower at the surface that contacted the glass plate, as compared to that exposed to the coagulant directly (Figs. 3(a) to 3(b)). During the coagulation process, as the cellulose solution contacted with the coagulant, solvent exchange occurs where the coagulant penetrates into the cellulose solution and at the same time the solvent (alkali and urea) diffusing out. The solvent will be removed out and left behind cellulose molecules due to the penetration of the coagulant into cellulose solution (Zhang *et al.* 2009, 2010b; Li et al. 2012). Therefore, the removal of the solvents left behind the pores. Hence, by increasing the PVA content, the solvent removal was enhanced and the pore size was increased. However, at the bottom side of the films there was no significant difference in film surface morphology. This is due to the fact that the contact of the coagulant was very slow, yielding very small pores and inducing a rolling effect. During the casting, a glass roller was used to roll the cellulose solution on the glass plate. The difference in the diffusion between solvents in a cellulose solution in a coagulation bath brings about a significant variation of the pore size between the surface and the bottom side of films (Ruan *et al.* 2004; Mao *et al.* 2006; Li *et al.* 2012).The surface was in direct contact with the coagulant, resulting in a larger pore size and coarser surface.

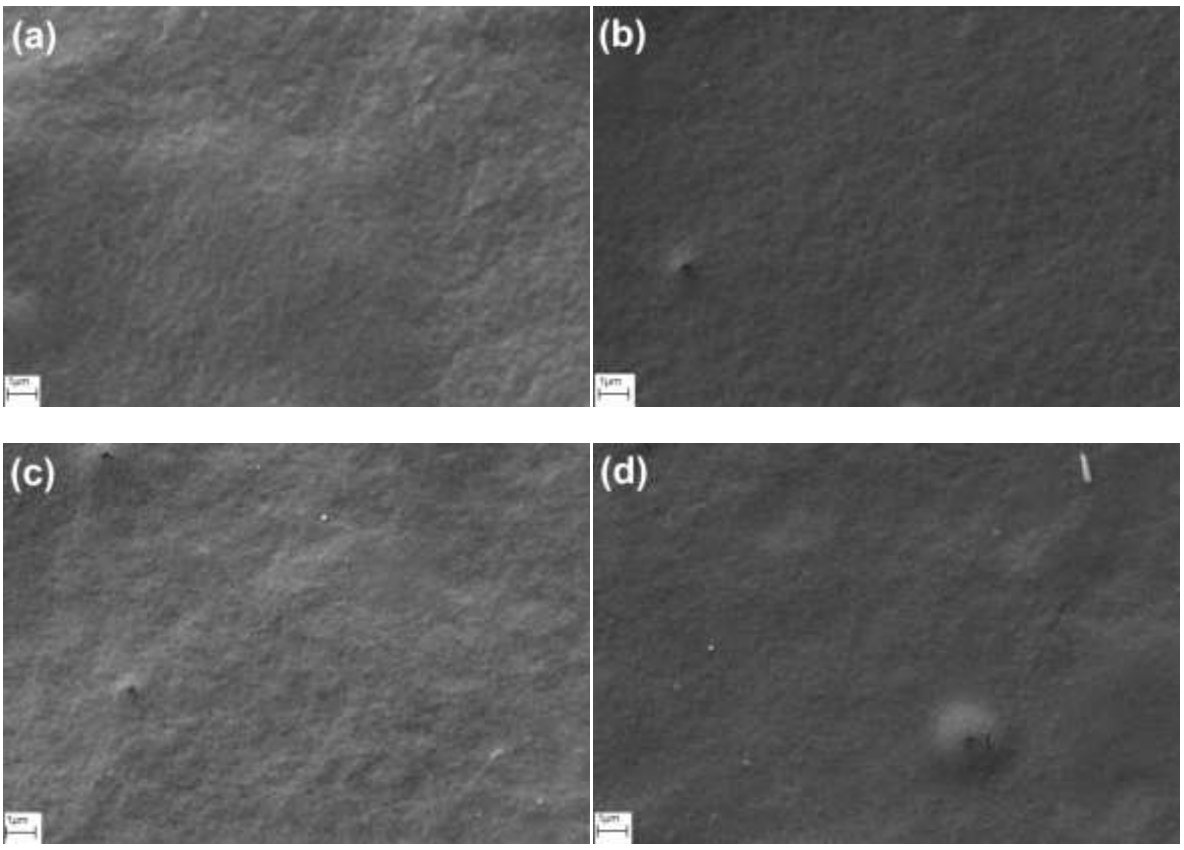

Fig. 4. SEM images of the bottom side of films (a) PVA0, (b) PVA1, (c) PVA5, and (d) PVA10

Transparency

The transmittance of the film samples at different CS/PVA ratios is presented in Fig. 5. All samples showed the lowest transmittance at a wavelength of 283 nm. This is due to the high energy absorption assigned to $\pi - \pi^*$ bonds present in the tail head of the polymer, which is influenced by its molecular weight (Fortunati *et al.* 2013). The transmittance of the CS/PVA films increased with increasing PVA content, and the highest transmittance of 45% was observed for the film with 10% PVA. The miscibility of the polymer can be explained from the transparency of the film produced. It may be due to the formation of hydrogen bonding between the hydroxyl groups of cellulose and those of PVA (Agarwal *et al.* 2013). Therefore, as the PVA content increased, more hydrogen bonds formed. Therefore, the increase in the transparency of films at higher PVA contents shows more clearly the miscibility of the polymer due to more interactions between cellulose and PVA.

As shown in the XRD results (Fig. 2), a decrease in the crystallinity index was observed as the PVA content increased. The crystalline region in the membrane affected the transparency of the film, which resulted in the loss of light transparency (Chang *et al.* 2010). In addition, the pore size of the samples also influenced the films' transparency. The addition of PVA to the cellulose solution resulted in an increase in the pore size of the film. The greater the porosity is, the easier it is for light to pass through the film, leading to higher transparency.

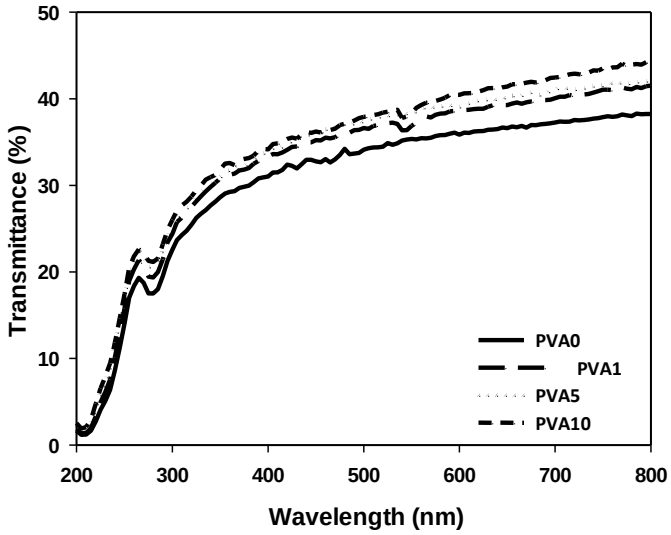

Fig. 5. Transmittance of films PVA0, PVA1, PVA5, and PVA10

Tensile Strength

The tensile strengths of conditioned neat cellulose and CS/PVA were evaluated and are reported in Fig. 6. The tensile index of the films decreased with increasing PVA content. There were interactions between cellulose and PVA, which involved the formation of interchain hydrogen bonds between hydroxyl groups of PVA and ether oxygen in cellulose (Sawatari and Kondo 1999). This will lead to softening effect due to the diffusion of water molecules into the mixed polymer. This may be traced quantitatively by observation of its accompanying mechanical effects, which reduced the tensile index of the film (Yamamura and Kuramoto 1959). The results can also be explained by

the SEM results, in which the addition of PVA led to increasing pore size. The greater the porosity is, the easier it is for the water molecule to diffuse into the structure of the films. The diffusion of water molecules resulted in softening of the film due to the breaking of hydrogen bonds during the diffusion (Yamamura and Kuramoto 1959). This can be demonstrated from the FTIR spectra, in which the intensity at wavelength 3200 to 3500 cm^{-1} due to OH stretching was increased. Therefore, it resulted in the reduction of the tensile strength of the film as the PVA content increased. The decrease of the tensile strength can also be explained by the decreasing degree of crystallinity of the CS/PVA films (Abd El-Kader *et al.* 2002).

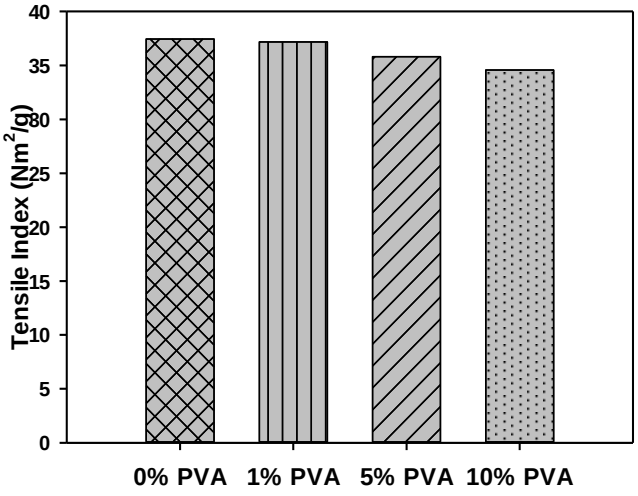

Fig. 6. Tensile index of CS/PVA films with different CS/PVA ratios

Printing and Ink Detachment

Figure 7(a) shows the CS/PVA film produced from the mixed cellulose/PVA solution *via* the casting method, while Fig. 7(b) shows the film sample after printing using a laser printer and the color remaining on the printed film. It has been reported that PVA is used in the printing industry as a binding agent, in which the addition of PVA provides excellent binding strength and improves the print quality (Matilainen *et al.* 2012). All the cellulose and CS/PVA films were printed and immersed in distilled water for ink detachment purposes.

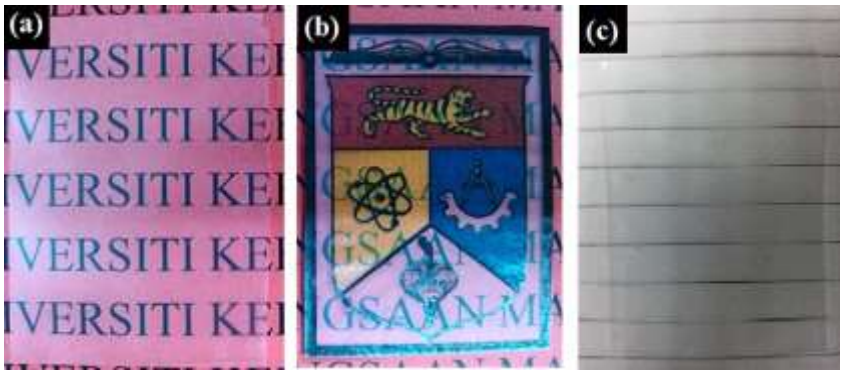

Fig. 7. Photograph of (a) CS/PVA film, (b) printed film, and (c) film after ink completely peeled off

Figure 7(c) shows that the film maintained its transparency after the ink was completely removed. During the ink detachment test, water acts as a wetting and swelling agent, wetting and softening the films. The swelling of cellulose during the process promotes the detachment of the ink pigments, so that the ink pigments can more easily be removed from the film structure (Borchardt *et al.* 1998). The ink printed on the PVA10 was the easiest to detach, followed by that on PVA5, PVA1, and PVA0. This may be due to the larger pore size of the films, as compared to other samples. Therefore, the ink pigments are easy to remove and these films can be reprinted repeatedly.

The scotch tape test was employed for estimating the adhesion strength of the ink on films. Figure 8(a) shows the printed film of PVA0 and PVA10; the ink on both printed films was removed using the tape test method. As can be seen in Fig. 8 (b) and (d), the ink was easier to remove from PVA10 (Fig. 8(d)) than it was from PVA0 (Fig. 8(b)). This may due to the pore size of PVA10, which is larger than that of PVA0. The pore size will affect the ink detachment because a larger pore size makes it easier for the ink to be detached using water.

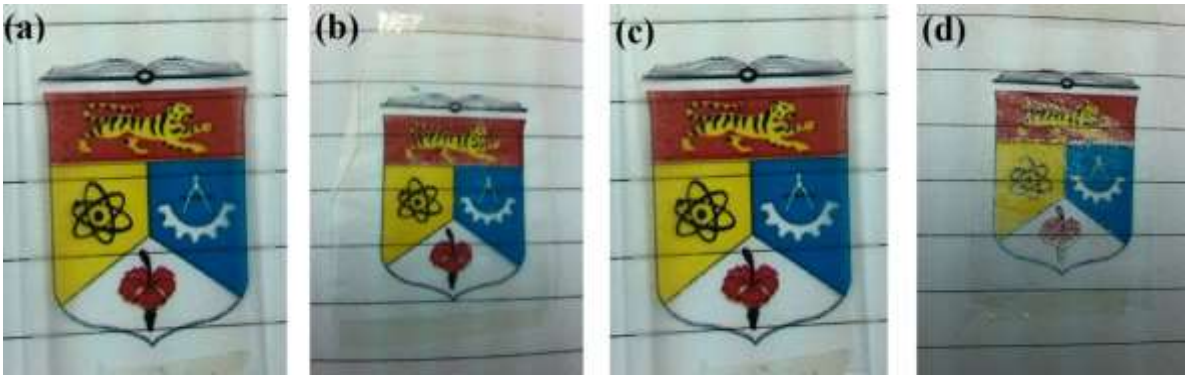

Fig. 8. Photograph of (a) printed PVA0 film, (b) ink detached from PVA0, (c) printed PVA10 film, and (d) ink detached from PVA10

CONCLUSIONS

1. Cellulose/PVA films with different CS/PVA ratios were prepared using the pre-cooled and casting method.
2. As the PVA content increased in the mixed polymer, the crystallinity decreased and the UV-Vis transmittance data showed that the transparency increased. From the SEM images, as can be observed from the top side of the film, which contacted the coagulant, the pore size of the film increased with increasing PVA content. However, as observed from the bottom side, which contacted the glass plate, the surface was smooth and the pore size was very small. The tensile strength properties of the film show the opposite trend, decreasing as PVA increases.
3. Both cellulose and cellulose/PVA films can be printed. However, the de-inking properties of the printable film showed that as the PVA content increased, it was easier to de-ink the film using water and to recycle the film, where the number of reuses can be as high as three.

ACKNOWLEDGMENTS

The authors are grateful for the support of the Universiti Kebangsaan Malaysia (UKM) for financial support (UKM-DLP-2011-036, LRGS/TD/2012/USM-UKM/PT/04, UKM-GUP-2011-227, ERGS/1/2012/STG05/UKM/01/4), and the Centre for Research and Instrumentation Management (CRIM) (UKM).

REFERENCES CITED

Abd El-Kader, K. A. M., Abdel Hamied, S. F., Mansour, A. B., El-Lawindy, A. M. Y., and El-Tantaway, F. (2002). "Effect of the molecular weights on the optical and mechanical properties of poly(vinyl alcohol) films," *Polym. Test.* 21(7), 847-850.

Abdul Khalil, H. P. S., Ireana Yusra, A. F., Bhat, A. H., and Jawaid, M. (2010). "Cell wall ultrastructure, anatomy, lignin distribution, and chemical composition of Malaysian cultivated kenaf fiber," *Ind. Crop. Prod.* 31(1), 113-121.

Agarwal, R., Sarwar Alam, M., and Gupta, B. (2013). "Polyvinyl alcohol-polyethylene oxide-carboxymethyl cellulose membranes for drug delivery," *J. Appl Polym. Sci.*129(6), 3728-3736.

Borchard, J. K., Miller, J. D, and Azevedo, M. A. D. (1998). "Office paper de-inking," *Curr. Opin. Colloid Interface Sci.* 3(4), 360-367.

Cai, J., Liu, Y., and Zhang, L. (2006). "Dilute dissolution properties of cellulose in LiOH/Urea aqueous system," *J. Polym. Sci., Part B: Polym. Phys.* 44(21), 3093-3101.

Chang, C., Zhang, L., Zhou, J., Zhang, L., and Kennedy, J. F. (2010). "Structure and properties of hydrogels prepared from cellulose in NaOH/urea aqueous solutions," *Carbohydr. Polym.* 82(1), 122-127.

Chia, C. H., Zakaria, S., Nguyen, K. L., and Abdullah, M. (2008). "Utilisation of unbleached kenaf fibers for the preparation of magnetic paper," *Ind. Crop. Prod.* 28(3), 333-339.

Chiaiese, P., Ruotolo, G., Di Matteo, A., De Santo Virzo, A., De Marco, A., and Filippon, E. (2011). "Cloning and expression analysis of kenaf (*Hibiscus cannabinus* L.) major lignin and cellulose biosynthesis gene sequences and polymer quantification during plant development," *Ind. Crop. Prod*. 34(1), 1072-1078.

Fortunati, E., Puglia, D., Monti, M., Santulli, C., Maniruzzaman, M., and Kenny, J. M. (2013). "Cellulose nanocrystals extracted from okra fibers in PVA nanocomposites," *J. Appl. Polym. Sci.* 128(5), 3220-3230.

Graupner, N., Herrmann, A. S., and Müssig, J. (2009). "Natural and man-made cellulose fibre-reinforced poly(lactic acid) (PLA) composites: An overview about mechanical characteristics and application areas," *Compos. Part A-Appl. Sci.* 40(6-7), 810-821.

Gupta, B., Agarwal. R., and Sarwal Alam, M. (2013). "Preparation and characterization of polyvinyl alcohol-polyethylene oxide-carbohymethyl cellulose blend membranes," *J. Appl Polym. Sci.* 127(2) , 1301-1308.

Ibrahim, M. M., Koschella, A., Kadry, G., and Heinze, T. (2013). "Evaluation of cellulose and carboxymethyl cellulose/poly(vinyl alcohol) membranes," *Carbohydr. Polym.* 95(1), 414-420.

Jin, H., Zha, C., and Gu, L. (2007). "Direct dissolution of cellulose in NaOH/thiourea/ urea aqueous solution," *Carbohydr. Res.* 342(6), 851-858.

Li, R., Zhang, L., and Xu, M. (2012). "Novel regenerated cellulose films prepared by coagulating with water: Structure and properties," *Carbohydr. Polym.* 87(1), 95-100.

Luo, X., and Zhang, L. (2013). "New solvents and functional materials prepared from cellulose solutions in alkali/urea aqueous system," *Food Res. Int*. 52(1), 387-400.

Mao, Y., Zhou, J., Cai, J., and Zhang, L. (2006). "Effects of coagulants on porous structure of membranes prepared from cellulose in NaOH/urea aqueous solution," *J. Membrane Sci.* 279(1-2), 246-255.

Matilainen, K., Hämäläinen, T., Savolainen, A., Sipiläinen-Malm, T., Peltonen, J., Erho, T., and Smolander, M. (2012). "Performance and penetration of laccase and ABTS inks on various printing substrates," *Colloid. Surface. B* 90(1), 119-128.

Mambelli, S., and Grandi, S. (1995). "Yield and quality of kenaf (*Hibiscus cannabinus* L.) stem as affected by harvest date and irrigation," *Ind. Crop. Prod.* 4(2), 97-104.

Pawde, S.M., Deshmukh., Kalim., and Parab, S. (2008). "Preparation and characterization of poly(vinyl alcohol) and gelatin blend films," *J. Appl Polym. Sci.* 109(2), 1328-1337.

Qiu, K., and Netravali, A.N. (2012). "Fabrication and characterization of biodegradable composites based on microfibrillated cellulose and polyvinyl alcohol," *Compos. Sci. Technol.* 72(13), 1588-1594.

Roy, S., and Bysakh, S. (2011). "Ultrafine PZT based ceramics synthesized by auto-ignition of metal–polymer gel: Enhanced sinterablity and higher remnant polarization," *Mater. Chem. Phys.* 126(3), 948-954.

Ruan, D., Zhang, L., Mao, Y., Zeng, M., and Li, X. (2004). "Microporous membranes prepared from cellulose in NaOH/thiourea aqueous solution," *J. Membrane Sci.* 241(2), 265-274.

Sawatari, C., and Kondo, T. (1999). "Interchain hydrogen bonds in blend films of poly(vinyl alcohol) and its derivatives with poly(ethylene oxide)," *Macromolecules* 32(6), 1949-1955.

Suryanegara, L., Nakagaito, A. N., and Yano, H. (2009). "The effect of crystallization of PLA on the thermal and mechanical properties of microfibrillated cellulose-reinforced PLA composites," *Compos. Sci. Technol.* 69(7-8), 1187-1192.

Wang, D., Shang, S. B, Song, Z. Q., and Lee, M. K. (2010). "Evaluation of microcrystalline cellulose prepared from kenaf fibers," *J. Ind. Eng. Chem.* 16(1), 152-156.

Wu, R. L., Wang, X. L., Li, F., Li, H. Z., and Wang, Y. Z. (2009). "Green composite films prepared from cellulose, starch and lignin in room-temperature ionic liquid," *Bioresour. Technol.* 100(9), 2569-2574.

Yamamura, H., and Kuramoto, N. (1959). "Diffusion-controlled mechanical properties of polyvinyl alcohol and polyvinyl formals," *J. Appl. Polym. Sci.* 2(4), 71-80.

Yang, G., Zhang, L., and Feng, H. (1999). "Role of polyethylene glycol in formation and structure of regenerated cellulose microporous membrane," *J. Membrane Sci.* 161(1-2), 31-40.

Zhang, H., Wu, J., Zhang, J., and He, J. (2005). "1-Allyl-3-methylimidazolium chloride room temperature ionic liquid: A new and powerful nonderivatizing solvent for cellulose," *Macromolecules* 38(20), 8272-8277.

Zhang, L., Ruan, D., and Gao, S. (2002). "Dissolution and regeneration of cellulose in NaOH/thiourea aqueous solution," *J. Polym. Sci. Pol. Phys.* 40(14), 1521-1529.

Zhang, S., Li, F. X., Yu, J. Y., and Hsieh, Y. L. (2010a). "Dissolution behaviour and solubility of cellulose in NaOH complex solution," *Carbohydr. Polym.* 81(3), 668-674.

Zhang, S., Li, F. X. and Yu, J. Y. (2010b). "Kinetics of cellulose regeneration from cellulose-NaOH/thiourea/urea/H_2O system," *Cell. Chem. Technol*. 45(9-10), 593-604.

Zhang, S., Fu, C. F., Li, F. X. Yu, J. Y. and Li-xia G. (2009). "Direct preparation of a novel membrane from unsubstituted cellulose in NaOH complex solution," *Iran Polym J.* 18(10), 767-776.

Article submitted: December 11, 2013; Peer review completed: January 12, 2014; Revised version received and accepted: January 29, 2014; Published: February 28, 2014.